EDGEWOOD

CHEMICAL BIOLOGICAL CENTER

U.S. ARMY RESEARCH, DEVELOPMENT AND ENGINEERING COMMAND

ECBC-TR-845

EVALUATION OF THE AIRIS STANDOFF HYPERSPECTRAL IMAGING SYSTEM

Ronald W. Miles

RESEARCH AND TECHNOLOGY DIRECTORATE

Melissa S. Hulet
Barry R. Williams

SCIENCE APPLICATIONS INTERNATIONAL CORPORATION
Gunpowder, MD 21010-0068

Rex K. Miyashiro

RESEARCH SUPPORT INSTRUMENTS, INC.
Lanham, MD 20706

William J. Marinelli

PHYSICAL SCIENCES, INC.
Andover, MA 01810

January 2011

ABERDEEN PROVING GROUND, MD 21010-5424

Disclaimer

The findings in this report are not to be construed as an official Department of the Army position unless so designated by other authorizing documents.

REPORT DOCUMENTATION PAGE

Form Approved
OMB No. 0704-0188

1. REPORT DATE *(DD-MM-YYYY)*	2. REPORT TYPE	3. DATES COVERED *(From - To)*
XX-01-2011	Final	Sep 2009 - Nov 2009

4. TITLE AND SUBTITLE

Evaluation of the AIRIS Standoff Hyperspectral Imaging System

5a. CONTRACT NUMBER

5b. GRANT NUMBER

5c. PROGRAM ELEMENT NUMBER

6. AUTHOR(S)

Miles, Ronald W. (ECBC); Hulet, Melissa S.; Williams, Barry R. (SAIC); Miyashiro, Rex K. (RSI); and Marinelli, William J. (PSI)

5d. PROJECT NUMBER
None

5e. TASK NUMBER

5f. WORK UNIT NUMBER

7. PERFORMING ORGANIZATION NAME(S) AND ADDRESS(ES)

DIR, ECBC, ATTN: RDCB-DRD-P, APG, MD 21010-5424
SAIC, P.O. Box 68, Gunpowder, MD 21010-0068
Research Support Instruments, Inc., 4325B Forbes Drive, Lanham, MD 20706
Physical Sciences, Inc., 20 New England Business Center, Andover, MA 01810

8. PERFORMING ORGANIZATION REPORT NUMBER
ECBC-TR-845

9. SPONSORING / MONITORING AGENCY NAME(S) AND ADDRESS(ES)

10. SPONSOR/MONITOR'S ACRONYM(S)

11. SPONSOR/MONITOR'S REPORT NUMBER(S)

12. DISTRIBUTION / AVAILABILITY STATEMENT

Approved for public release; distribution is unlimited.

13. SUPPLEMENTARY NOTES

14. ABSTRACT

The ability of the AIRIS (Physical Sciences, Inc., Andover, MA) standoff sensor to detect chemical agents was examined in a series of laboratory measurements. Agents were passed through a flow cell, which was viewed against a blackbody that defined the thermal background. The cell was translated through the sensor's field of regard to simulate the impact of cloud motion on detection capability. This experiment used agent column densities and background thermal contrasts that were representative of those identified in the Commercial Joint Service Lightweight Standoff Chemical Agent Detector (JSLSCAD) specifications. The sensor demonstrated the ability to detect the agents GB and GD at or above JSLSCAD threshold conditions. The ability to detect HD at threshold levels was marginally achieved, but the results were compromised by experimental limitations. Analysis of the test results using the spectra of agents that were not tested suggests similar capability could be expected.

15. SUBJECT TERMS

AIRIS	Hyperspectral	Infrared	Chemical	Agent
Passive	Standoff	Detection	Vapor-phase	JSLSCAD

16. SECURITY CLASSIFICATION OF:			17. LIMITATION OF ABSTRACT	18. NUMBER OF PAGES	19a. NAME OF RESPONSIBLE PERSON
					Sandra J. Johnson
a. REPORT	b. ABSTRACT	c. THIS PAGE			19b. TELEPHONE NUMBER *(include area code)*
U	U	U	UL	24	(410) 436-2914

Blank

PREFACE

The work was started in September 2009 and completed in November 2009.

The use of either trade or manufacturers' names in this report does not constitute an official endorsement of any commercial products.

This report has been approved for public release. Registered users should request additional copies from the Defense Technical Information Center; unregistered users should direct such requests to the National Technical Information Service.

Acknowledgments

The authors acknowledge Alan Samuels, James O. Jensen (U.S. Army Edgewood Chemical Biological Center), and Steve Kolodzey (Joint Program Mananger for NBC Contamination Avoidance System Engineering and Standoff Detection) for their support conducting these tests.

Blank

CONTENTS

FIGURES

TABLES

EVALUATION OF THE AIRIS STANDOFF HYPERSPECTRAL IMAGING SYSTEM

1. INTRODUCTION

1.1 Background

Passive standoff detection of chemical agent vapors and aerosols has long been a tenet of chemical and biological defense. Starting with the M21 Remote Sensing Chemical Agent Alarm, which was first fielded in 1996, and continuing with the development of the Joint Service Lightweight Standoff Chemical Agent Detector (JSLSCAD), the use of passive infrared (IR) spectral detection of agent vapors has been the primary approach for detecting these threats, nominally at ranges up to 5 km.

In 1997 and continuing through the completion of the first integrated prototype in 2005, the Adaptive Infrared Imaging Spectroradiometer - Wide Area Detector (AIRIS-WAD) was developed by Physical Sciences Inc. to be the first imaging passive standoff IR chemical agent vapor sensor. From 2005 to 2009, the AIRIS sensor was tested in a variety of ground and airborne configurations to detect chemical vapor and aerosol simulants at locations including Defense Science and Technology Laboratory Porton Down, Dugway Proving Ground, the U.S. Army Redstone Technical Test Center, and Naval Surface Warfare Center Dahlgren. In 2009, the JPM NBC CA funded the development of a capability to evaluate the AIRIS and similar sensors against chemical agents at the U.S. Army Edgewood Chemical Biological Center (ECBC). Also in 2009, two AIRIS-WAD sensors were converted into a hardened variant as a candidate technology for insertion into the Next Generation Chemical Standoff Detection program. This report describes the testing of this AIRIS variant using the ECBC capability.

1.2 Objectives and Scope

The objective of the tests was to determine the capability of the AIRIS sensor to detect known column densities of chemical warfare (CW) agents against a known thermal background in a laboratory setting. The laboratory tests were designed to simulate typical cloud motion. The tests were limited to the agent vapors GB, GD, and HD. The test metrics were defined to be those developed for the JSLSCAD sensor.

2. DETECTION PHENOMENOLOGY AND METRICS

The phenomenology used for passive hyperspectral detection of chemical vapors is based on a radiative transfer mechanism, components of which are shown schematically in Figure 1. The figure depicts thermal IR radiation from the background passing through the target vapor cloud, where it is modified as a function of wavelength by the discrete IR absorption bands of the target chemical. Equation 1 is a simplified expression showing that the radiance measured at the sensor (N_D) is comprised of three components:

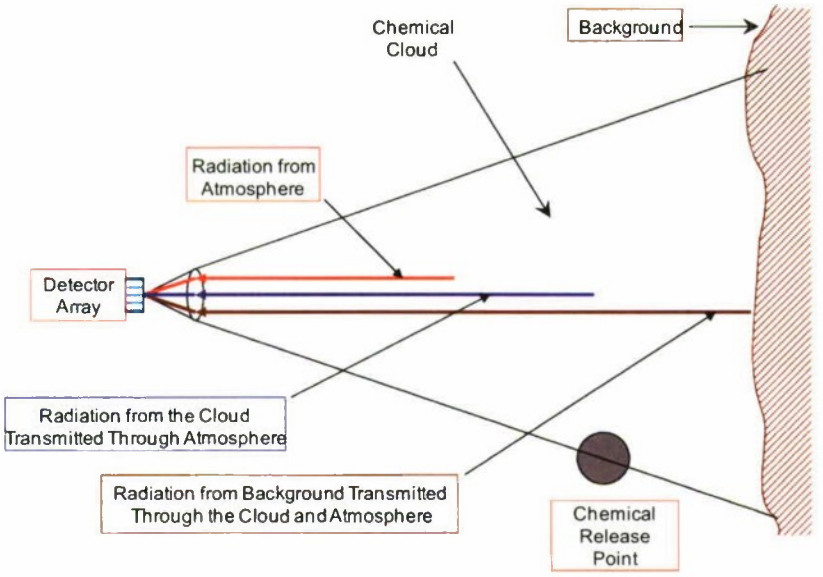

Figure 1. Physical depiction of the components of the radiative transfer mechanism governing vapor detection.

- The background radiation (N_B), modulated by the target cloud transmission ($1-\alpha\rho$) and the atmospheric transmission (τ_A) between the cloud and sensor.

- The target cloud radiation ($N_A\alpha\rho$) modulated by the same atmospheric transmission.

- The direct thermal emission of the atmosphere along the path from the cloud to the sensor ($N_A(1-\tau_A)$)

$$N_D = N_B\tau_A(1-\alpha\rho) + N_A\tau_A\alpha\rho + N_A(1-\tau_A) \qquad (1)$$

The differential radiance measured at the sensor due to the presence of the cloud is given by the expression (eq 2):

$$dN = \alpha\tau_A(N_A - N_B)d\rho \qquad (2)$$

Equation 2 shows that the differential radiance (dN) due to the presence of the cloud is proportional to the target compound extinction coefficient, α, and column density, ρ, as well as the difference between the atmospheric and the background radiances ($N_A - N_B$), or so called "delta-T" (ΔT). Thus, the experiments used carefully controlled values of ρ and ΔT for each agent tested to characterize the sensor's ability to measure dN and subsequently, infer the presence of the target agent.

Metrics for agent deteetion have most recently been established in the document Commercial JSLSCAD, which was published by the Joint Program Manager for NBC Contamination Avoidanee, August 2003. These specifications are provided in Table 1. Though not explicitly stated in the specifications, commonly these quantities are used in conjunction with an assumed ΔT of 3K. These specifications form the basis for defining the test conditions used in evaluating the sensor's performance.

Table 1. Commercial JSLSCAD Detection Limit Specifications.

Agent		ρ (mg/m2) (Threshold)	ρ (mg/m2) (Objective)
Class	**Type**		
NERVE	GA	135	14
	GB	135	14
	GF	135	14
	GD	135	14
	VX	135	14
	VX	135	14
BLISTER	HD	3,300	1,650
	L	3,300	1,650
	HN3	3,300	1,650
BLOOD	AC	---	6,600
	CK	---	6,600

3. DESCRIPTION OF THE AIRIS SENSOR

The AIRIS-WAD technical concept is based on the insertion of a tunable Fabry-Perot interferometer (etalon) into the field of view of an IR focal plane array (FPA). The IR FPA views the far field through the piezoelectric-aetuated etalon, whieh is placed in an afoeal region of the optical train. This tunable etalon is operated in low order (mirror spacing comparable to the wavelength of the light transmitted) and functions as a band pass filter, which selects the wavelength viewed by the FPA. The optical configuration affords a wide field of view (32° x 32°), high optical throughput (>60%), and broad wavelength (8 - 11 μm) coverage at high spectral resolution (10 cm^{-1}). Fore-optics and integrated blackbody calibration sources enable control of the sensor's field-of-regard, as well as absolute radiometric calibration of the data. The 256 x 256 pixel format of the array provides 2.2 milliradian (mrad) angular resolution or 11 m at 5 km range. A full hyperspectral acquisition can be achieved in <200 ms with this system.

Physical Sciences Inc. (the technology developer) has entered into a Technology Development Agreement with Smiths Detection under which the two organizations jointly fund improvements in the capability and reliability of the technology with the goal of insertion into Next Generation Chemical Standoff Detection (NGCSD) program. Under this effort, two existing sensor units were outfitted with improved cooling to meet environmental requirements, a weatherproof sealed housing, and a new operator display unit/processor in the form of a Panasonic Toughbook 30 laptop computer with a touch screen display. This process was enabled by a Cooperative Research and Development Agreement (CRADA) signed between PSI and ECBC. Figure 2 shows photographs of the system in the configuration as tested in July 2009 at the CBDEWS Operational Demonstration.

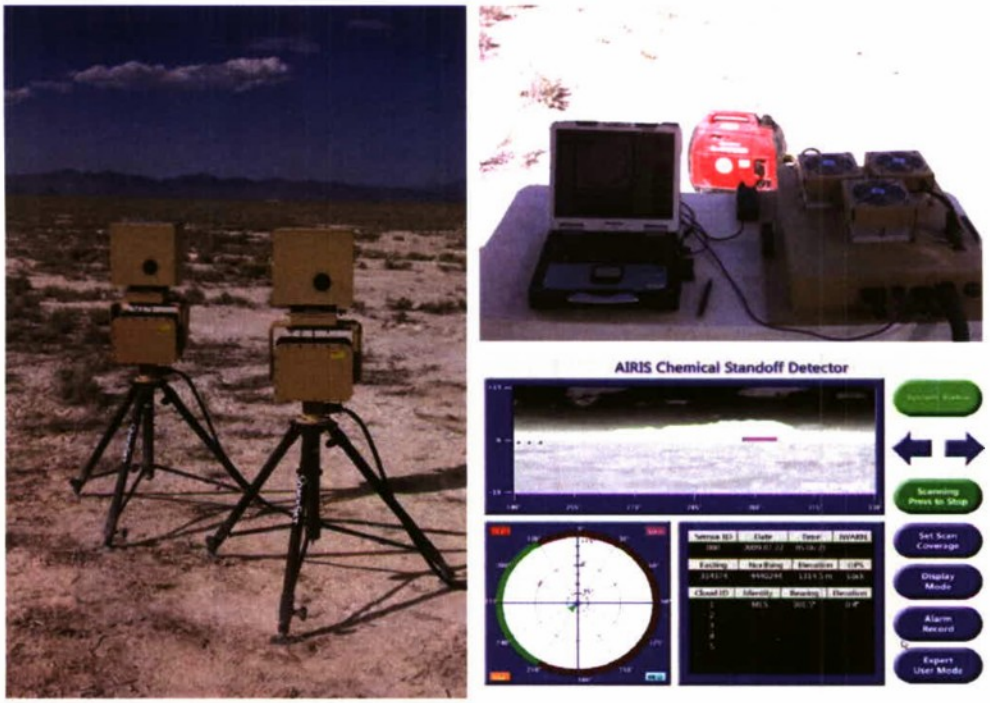

Figure 2. Photographs of the two AIRIS prototypes (left), notebook computer controller, power supply and generator used to operate each unit (top right), and screen shot of MES detection during the CBDEWS Operational Demonstration at Dugway Proving Grounds in July 2009 (lower right).

4. EXPERIMENT APPARATUS AND METHODS

4.1 Overview

The measurements were conducted in the Quantitative Fourier Transform Infrared (FTIR) Laboratory located in Building 3400 at ECBC. The experimental configuration is shown schematically in Figure 3. It comprises a bench-mounted AIRIS sensor looking through a gas flow

chamber (flow cell) at an enlarged blackbody source. The flow cell and the blackbody are located within a fume hood. The fume hood sash was open for the tests. The flow cell is mounted on a linear translation stage. For each test, the flow cell is traversed in azimuth at rates that simulate the motion of the cloud through the field of view of the sensor.

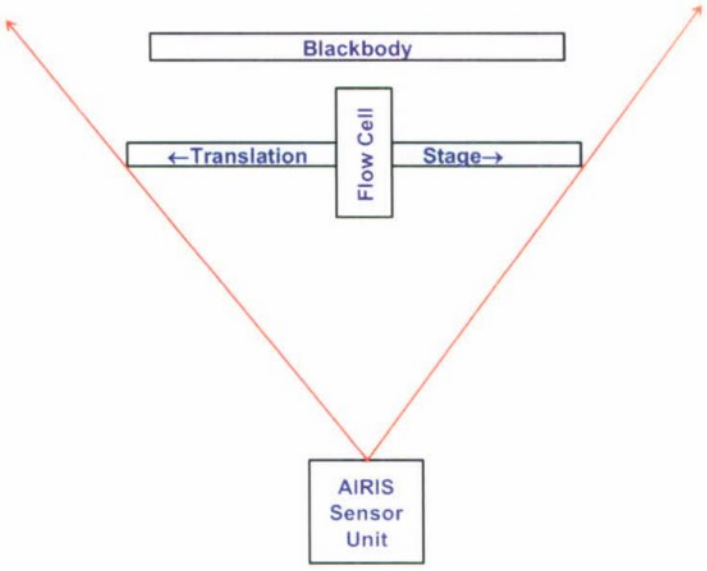

Figure 3. Schematic diagram of the test configuration.

4.2 Flow Cell and Blackbody Background

The flow cell and enlarged blackbody source are shown in Figure 4. Known mass flow rates of agent, diluted in N_2, were continuously passed through a 50 cm long by 10 cm diameter glass-gas flow cell equipped with flat circular zinc selenide windows on each end. The flow cell was mounted on a computer controlled linear actuator that traversed the cell at a fixed rate across the front of an enlarged blackbody background. The linear actuator is an aluminum platform that is driven by a worm gear rotated by a computer controlled stepper motor (Velmex Inc., Bloomfield, NY, Model 30 BiSlide Assembly). The fixture to mount the flow cell on the linear actuator was designed and manufactured at ECBC.

Continuous alignment of the cell and sensor optical axes was accomplished by using an alignment rod between the cell and the front of the sensor. The cell was able to freely rotate in its mount, allowing the rod to turn the cell and maintain alignment between the sensor's field of view and the cell's optical axis. Class *A* Resistance Thermal Devices (RTD) (Omega Engineering, Inc., Bridgeport, CT, Part Number: SA1-RTD) were placed at the points where gas enters and exits the cell. The two values were averaged to estimate the gas temperature in the cell.

An enlarged thermal blackbody source was used as the background. It was constructed using two aluminum plates, aluminum frame and support. The assembly has a total

radiating area of 0.74 m^2 (8 ft^2 area: 24 in. high x 48 in. wide). The source's aluminum plate surfaces are coated with high emissivity paint: literature values range from $0.92 < \varepsilon < 0.96$ in the IR range. Kapton film resistive heaters (Omega Engineering, Inc., Bridgeport, CT) Part Number: KH-1212/(5)-P) contacted the back of the plates and were interfaced with Proportional-Integral-Derivative (PID) controllers to achieve and maintain accurate and precise surface temperatures. Class A RTD temperature sensors on the source surface provided feedback for the closed loop control system.

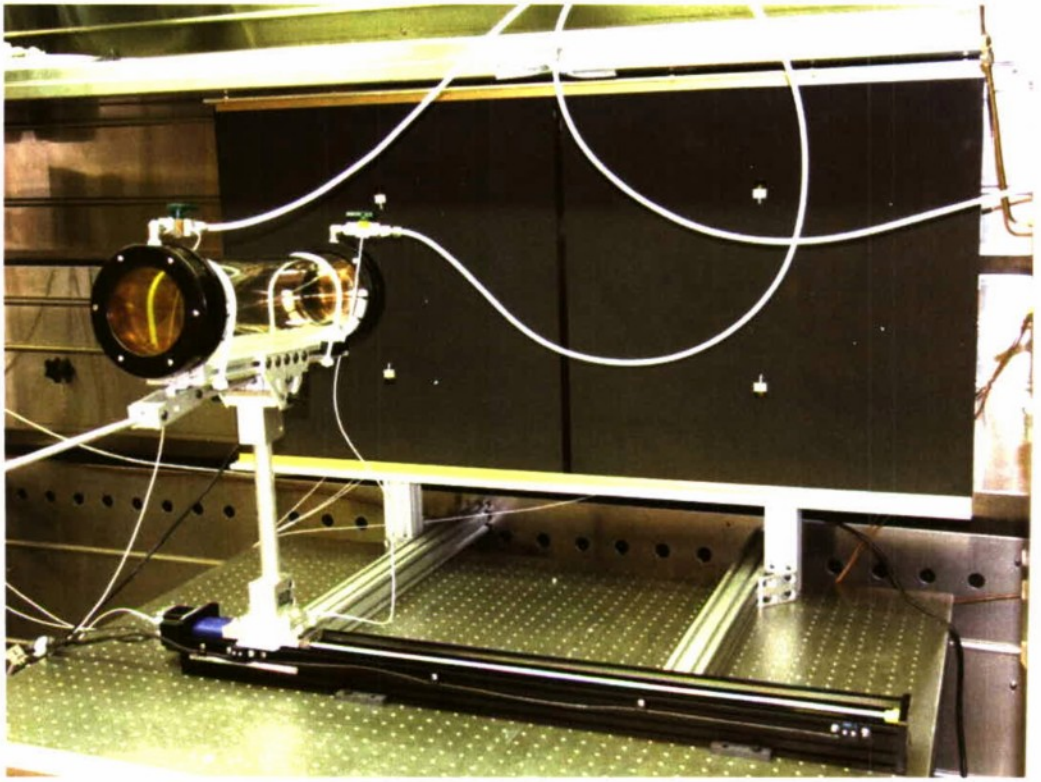

Figure 4. Photograph of flow cell in the foreground with enlarged blackbody source in the background. The alignment rod is shown attached below the cell.

4.3 Sample Preparation and Delivery

The system used to generate the continuous vapor stream was an adaptation of the saturator cell (Glassblowers Inc., Turnersville, NJ) method developed at ECBC for measuring the volatility of CW agent related compounds.[1] The method, modified to generate continuous streams of chemical compounds for obtaining quantitative vapor-phase IR spectra, has been used to measure the absorption coefficients of benzene, as well as a variety of CW agent related compounds. The development of this method has been described in a previous ECBC technical report.[2]

The saturator cell passes a stream of nitrogen carrier gas, obtained from the boil-off of a bulk liquid nitrogen tank, across a conical alumina wicking mechanism in a glass holder filled with the analyte. A saturated vapor-liquid equilibrium of the analyte on the downstream side of the saturator cell results, with the concentration of the analyte determined by the temperature of the liquid phase. By suspending the saturator cell in a constant temperature bath, the concentration of the analyte can be predicted by its vapor pressure at the temperature of the bath. The apparatus used in the Quantitative FTIR Laboratory uses a Brooks Model 5850S (Brooks Instrument Co., Hatfield, PA) mass flow controller to maintain a constant flow to the saturator cell, along with a second mass flow controller to add diluent to the stream, providing an additional means of adjusting the concentration. A photograph of the saturator system is shown in Figure 5. Linearity of the S series mass flow controllers is adjusted using a second order polynomial, resulting in accuracies of approximately 1% or better of rate at flows ≥25% of full scale. The flow from the saturator was continuously monitored using a Bruker Model IFS/66V FTIR equipped with a variable path White cell. The FTIR and white cell are shown in Figure 5.

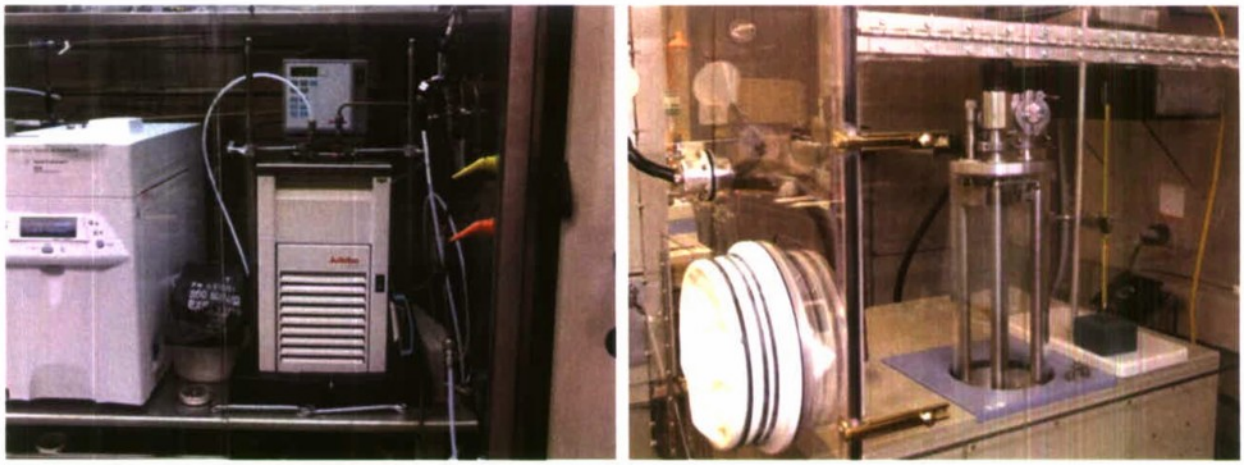

Figure 5. Saturator system used to introduce agent flows into the sample absorption cell (left) and FTIR used to monitor the agent concentrations during the measurements (right).

Before the compounds to be measured were added to the saturator cell, their purities were checked by Nuclear Magnetic Resonance (NMR) Spectroscopy and gas chromatography-mass spectrometry (GC-MS). The primary method of determining the actual mass flow rate of the compounds from the saturator cells, and thus their downstream concentrations, was by weighing the saturator cell at the beginning and end of the measurement series. A secondary method sampled the vapor by thermal desorption gas chromatography (TD-GC).

4.4 Sensor Configuration

For these measurements the AIRIS sensor was mounted on a lab bench opposite the fume hood, with the sensor's entrance window located approximately 1.6 m (63 in.) from the cell's front window. The optical axes of the sensor and the cell were about the same height from the floor and vertically centered on the blackbody, with the sensor pointed at the mid-point of the blackbody.

The AIRIS unit could be configured to detect four compounds simultaneously with its real time processor. In these measurements, the sensor was loaded with the spectra of the agents GB, GD, HD, and Lewisite, though Lewisite was not tested in these measurements. The tracer R134a, which was used to validate sensor operation prior to conducting measurements, was loaded into an alternate measurement channel. The spectra of these materials was obtained from the PNNL spectral database[3] and from ECBC technical reports,[4-6] normalized to the peak value within the 8.0 to 11.0 μm (nominal 900 to 1250 cm^{-1}) spectral range, and degraded to the 10 cm^{-1} spectral resolution of the AIRIS sensor. These spectra are shown in Figures 6 and 7.

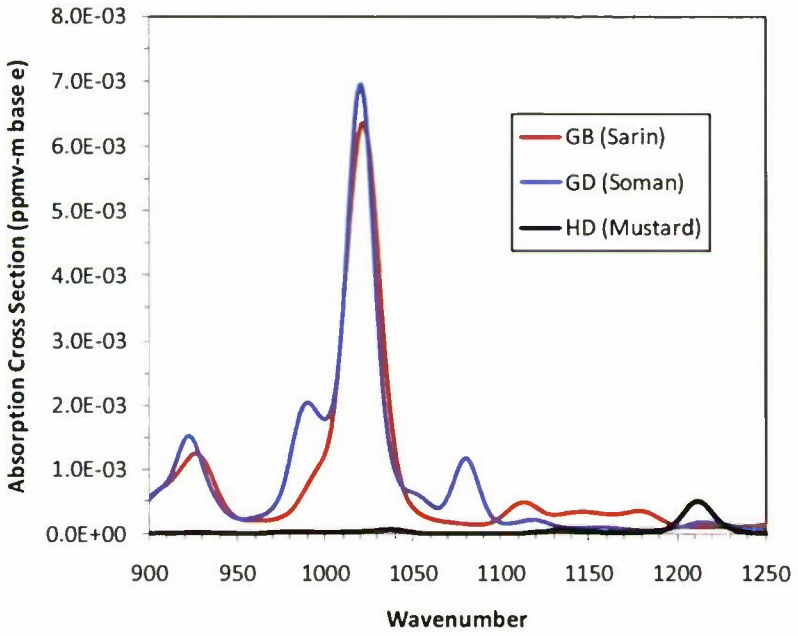

Figure 6. IR absorption spectra of GB, GD, and HD used in the measurements.

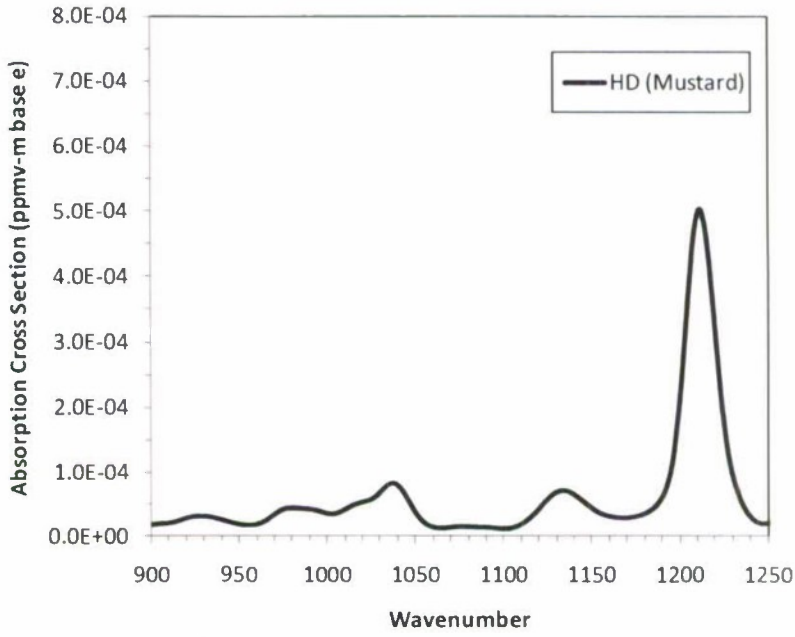

Figure 7. Expanded scale for the IR absorption spectrum of HD used in the measurements.

4.5 Experimental Procedures

The experiment measurements were conducted under conditions of steady state flow and steady state background blackbody temperature. Of the two, steady state flow of the agent took the longest time to reach equilibrium, extending intervals between tests. For each "test run," a selected combination of agent concentration and background blackbody temperature (see Table 2), the cell was traversed from left to right across the field of regard of the sensor. The cell traverse speed of 2 mm/s was established to approximate the same angular rate of change through the sensor's field of view as would be expected from a cloud moving at 2 m/s on the test range at a distance of 2 km or angular rate of 1 mrad/s. The total traverse length of the linear actuator is 76 cm, and at a speed of 2 mm/s, it takes approximately 380 s, or 6.35 min for the cell to traverse the entire length, thus determining the time of a test run. The cell's clear aperture of 10 cm simulates a "cloud", which scales to approximately 100 m at 2 km range.

The AIRIS has the ability to scan 360° in 30° sectors. For this test the sensor was operated in single scan mode (i.e., the sensor rotation fixed). In this mode, the sensor acquires data and returns the result of a scene interrogation every 10 s allowing 38 independent interrogations per test run.

The experiment procedures were conducted by fixing the cell concentration and then varying the background temperature. The large thermal mass of the blackbody required that the background temperature be ramped up for one concentration and then subsequently ramped down for the next concentration. See Table 2 for sequence of test runs. Limitations from saturator equilibrium times and safety requirements within the facility allowed only one agent series to be measured in an 8 h work period.

For HD, and to a lesser extent GD, the maximum vapor pressure of the agent achievable under laboratory operating conditions was not sufficient to achieve the threshold column densities defined in Table 1 for the 50 cm path length cell used in the measurements. The maximum column density of HD that could be achieved experimentally was 256 mg/m^2 compared to the threshold value of 3,300 mg/m^2. Following from eq 2, under these conditions the background temperature was increased until $\rho\Delta T$ values that approximated the product of the target thresholds from Table 1 and a ΔT of 3K were achieved. This constraint required that background temperatures as great as 96 °C be used in the measurements.

Standard detection thresholds for the AIRIS, previously established for simulant detection in the field, were used for the detection of agents in the laboratory. To separate false alarm issues from detection limitations, and because the artificial backgrounds present in the fume hood could be sources of false alarms, thresholds for all other species in the target set except for the agent under investigation were set to their maximum values.

4.6 Data Products

Several types of data are available for the evaluation of the sensor. The sensor's real time processor provides an IR image of the scene in which detected target pixels are indicated by a bounded set of pixels, which are color coded to indicate agent type. An image of the display screen with this data is captured every second and inserted into an MPEG movie, which can be viewed after the test is completed. The sensor's performance log provides data on system operating parameters, as well as the centroid and extents in azimuth and elevation of the detected cloud. This data is logged in CSV format to facilitate insertion into spreadsheets for analysis. Each detection event also produces an NBC-1 warning message, which is logged in a separate file. Finally, each scan produces a series of JPEG images of the scene, one per target compound, showing the pixel level detection of the targets in the scene. Sample data of the JPEG imagery for detection of all three target compounds (as well as Lewisite) are shown in Figure 8. These images are date/time stamped to aid in analysis. In addition to these processed data products, the sensor's raw data was archived for post analysis.

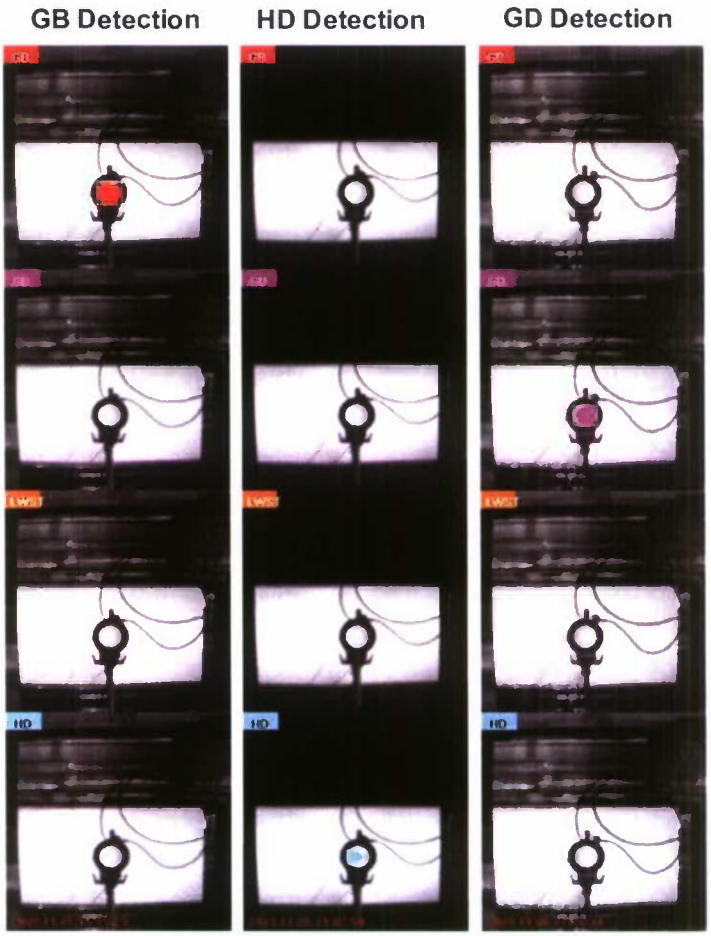

Figure 8. Sample JPEG images of detection events for GB, GD, and HD. Colored pixels marked as target detection are color coded to the color that highlights the agent abbreviation in the top left of each JPEG image.

5. TEST RESULTS AND DISCUSSION

Data from the JPEG imagery was used to determine the detection capability. The imagery was divided into three categories:

- Good (Green) - detection of the vapor in the cell was persistent throughout the cell aperture for approximately the entire duration of the test event.

- Fair (Yellow) - the detection of the agent vapor in the cell only partially filled its aperture or was not persistent throughout the course of the test event.

- Poor (Red) - no detection of the agent vapor in the cell was observed during the test event.

This detection data was tabulated as a function of the product of the thermal contrast (Kelvin) and the agent column density (mg/m^2), which is obtained from the product of the concentration measured by the FTIR sensor and the cell length (50 cm).

The data from all measurements conducted in the test series is shown in Table 2. It comprises 29 measurement events, of which three were mistakenly conducted using the wrong target spectrum for GD and were discarded. This data is also represented graphically in Figures 9 to 11. These figures show the thermal contrast, ΔT, for the data points in each agent series plotted as a function of the column density of agent, ρ, in the cell. Each data point is color coded for detection quality using the key defined above. Also plotted in each figure is a line defining the product of the threshold column density for the agent from Table 1 with a ΔT of 3K. In this representation of the specifications values of $\rho\Delta T$ exceeding those defined by the line should be detected by a sensor meeting the specifications.

The data for GB and GD indicate good detection capability compared to the respective standards. The data for HD is much more limited in scope as a result of the limited vapor pressure of HD at ambient temperatures and the short length of the flow cell (i.e., the maximum column density of HD that could be obtained from the apparatus was 256 mg/m^2 compared to the detection limit specification of 3,300 mg/m^2). This experiment limitation required that the background temperature be increased such that the $\rho\Delta T$ product approached, or exceeded, 9,900 mg/m^2 K, which is the product of 3K with the 3,300 mg/m^2 detection limit from Table 1.

To achieve the appropriate $\rho\Delta T$ conditions the blackbody temperature needed to be increased to values as high as 96 °C. This temperature is much higher than is expected under any set of operating conditions and required a reduction in the sensor's integration time to prevent saturation of pixels due to the high radiant flux. A concurrent reduction in system sensitivity results from this reduction in integration time. This reduction in system sensitivity is reflected in the data shown in Figure 11, where the capability to detect HD is marginal for the data point just above the JSLSCAD HD $\rho\Delta T$ specification line.

Table 2. Test Data Summary.

Experiment Conditions												Detection	Sensor Operation					Calibration	
Date	Experiment Name	Agent Tested	Agent Concentration (mg/m3)	Column Density (mg/m2)	Initial Gas Temperature (deg C)	Final Gas Temperature (deg C)	Initial Background Temperature (deg C)	Final Background Temperature (deg C)	Acquisition Start Time (UTC)	Acquisition End Time (UTC)	Delta T (deg C)	Quality (Green, Yellow, Red)	Integration Time (us)	GB Threshold	GD Threshold	Lewisite Threshold	HD Threshold	Blackbody Low Temperature (deg C)	Blackbody High Temperature (deg C)
GB Test Data																			
4-Nov-09	02GB1300T03	GB	1273	636.5	23.7	23.6	26.8	26.8	18:53:00	18:59:00	3.15	Green	620	2	255	255	255	15	40
4-Nov-09	03GB1300T06	GB	1273	636.5	23.5	23.7	29.6	29.6	19:09:00	19:15:20	6.00	Green	620	2	255	255	255	15	40
4-Nov-09	04GB1300T12	GB	1280	640	23.8	23.8	35.6	35.6	19:27:00	19:33:20	11.80	Green	620	2	255	255	255	15	40
4-Nov-09	05GB1000T03	GB	1000	500	23.7	23.7	26.7	26.7	20:02:00	20:08:20	3.00	Green	820	2	255	255	255	15	40
5-Nov-09	06GB1000T06	GB	1000	500	23.9	24.0	29.7	29.7	12:56:00	13:02:20	5.75	Green	620	2	255	255	255	15	40
5-Nov-09	07GB1000T12	GB	1000	500	24.0	24.1	35.9	35.9	13:09:00	13:15:20	11.85	Green	620	2	255	255	255	15	40
5-Nov-09	08GB0600T12	GB	600	300	24.2	24.4	38.0	36.0	13:26:00	13:32:15	11.70	Green	620	2	255	255	255	15	40
5-Nov-09	09GB0600T06	GB	600	300	24.3	24.3	30.5	30.4	13:57:00	14:03:15	6.15	Green	620	2	255	255	255	15	40
5-Nov-09	10GB0600T03	GB	600	300	24.3	24.4	27.5	27.5	14:17:00	14:23:15	3.15	Green	620	2	255	255	255	15	40
5-Nov-09	11GB0600T01	GB	600	300	24.4	24.4	25.5	25.5	14:41:00	14:47:15	1.10	Green	620	2	255	255	255	15	40
5-Nov-09	12GB0300T01	GB	286	143	24.5	24.5	25.5	25.5	14:57:00	15:03:15	1.00	Yellow	620	2	255	255	255	15	40
5-Nov-09	13GB0300T03	GB	286	143	24.3	24.5	28.2	27.6	15:13:00	15:19:20	3.50	Green	620	2	255	255	255	15	40
5-Nov-09	14GB0300T06	GB	286	143	24.2	24.2	31.0	30.8	15:28:00	15:34:00	6.70	Green	620	2	255	255	255	15	40
HD Test Data																			
5-Nov-09	15HD0500T30	HD	512	256	25.7	26.2	54.0	54.0	18:22:00	18:28:15	28.05	Yellow	620	255	255	255	1	15	50
5-Nov-09	16HD0500T50	HD	512	256	26.3	26.5	76.0	76.0	18:36:00	18:42:15	49.60	Yellow	620	255	255	255	1	15	50
5-Nov-09	17HD0500T50	HD	512	256	26.5	26.7	76.0	76.0	18:46:00	18:52:20	49.40	Yellow	620	255	255	255	1	15	50
5-Nov-09	18HD0500T70	HD	512	256	27.2	27.6	96.0	96.0	19:00:00	19:06:20	68.60	Green	620	255	255	255	1	15	50
5-Nov-09	19HD0500T70	HD	512	256	28.2	29.5	96.0	96.0	19:31:00	19:37:15	67.15	Green	620	255	255	255	1	15	70
GD Test Data																			
6-Nov-09	20GD0300T03	GD	302	151	24.0	23.9	26.5	26.5	14:17:00	14:23:15	2.55	*Wrong Spectrum	620	255	2	255	255	15	40
6-Nov-09	21GD0300T03	GD	302	151	23.8	23.7	27.0	27.0	14:29:00	14:35:20	3.25	*Wrong Spectrum	620	255	2	255	255	15	40
6-Nov-09	22GD0300T06	GD	302	151	23.8	23.8	30.0	30.0	14:59:00	15:05:20	6.2	*Wrong Spectrum	620	255	2	255	255	15	40
6-Nov-09	23GD0300T12	GD	302	151	24.1	24.2	36.0	36.0	16:29:00	16:35:15	11.85	Green	620	255	2	255	255	15	40
6-Nov-09	24GD0300T06	GD	302	151	24.2	24.2	30.2	30.2	16:51:00	16:57:15	6	Green	620	255	2	255	255	15	40
6-Nov-09	25GD0300T03	GD	302	151	24.2	24.1	27.2	27.2	17:14:00	17:20:15	3.05	Green	620	255	2	255	255	15	40
6-Nov-09	26GD0300T01	GD	302	151	24.0	23.9	25.2	25.2	17:37:00	17:43:15	1.25	Red	620	255	2	255	255	15	40
6-Nov-09	27GD0150T03	GD	152	76	23.7	23.7	27.1	26.9	17:56:00	18:02:15	3.3	Yellow	820	255	2	255	255	15	40
6-Nov-09	28GD0150T06	GD	152	76	23.6	23.6	30.0	30.0	18:12:00	18:18:15	6.4	Green	620	255	2	255	255	15	40
6-Nov-09	29GD0150T12	GD	152	76	23.6	23.6	36.0	36.0	18:22:00	18:28:15	12.4	Green	820	255	2	255	255	15	40
6-Nov-09	30GD0150T18	GD	152	76	23.6	23.6	42.0	42.0	18:34:00	18:40:15	18.4	Green	620	255	2	255	255	15	40

* Wrong Spectrum - incorrect spectrum for GD was initially loaded into the target spectrum library.

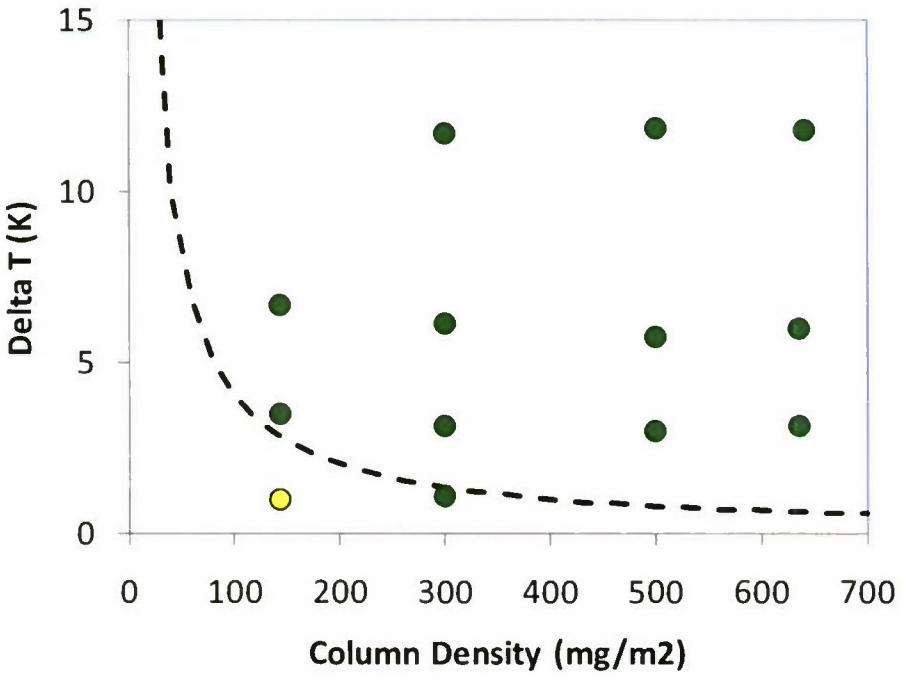

Figure 9. Graphical representation of test data (symbols) showing detection quality as a function of column density and ΔT for GB with JSLSCAD threshold limit (dashed line).

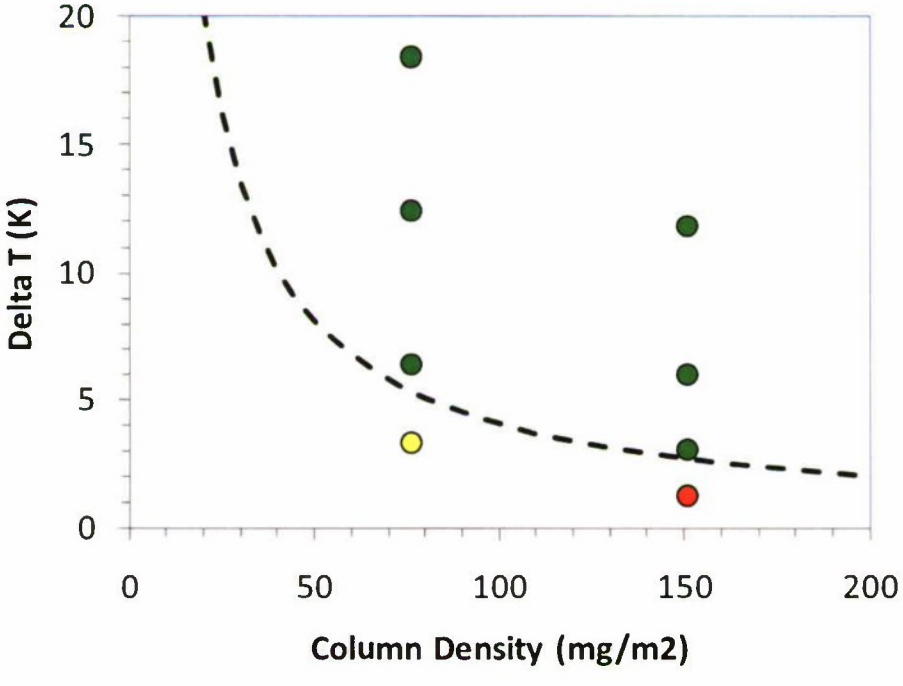

Figure 10. Graphical representation of test data (symbols) showing detection quality as a function of column density and ΔT for GD with JSLSCAD threshold limit (dashed line).

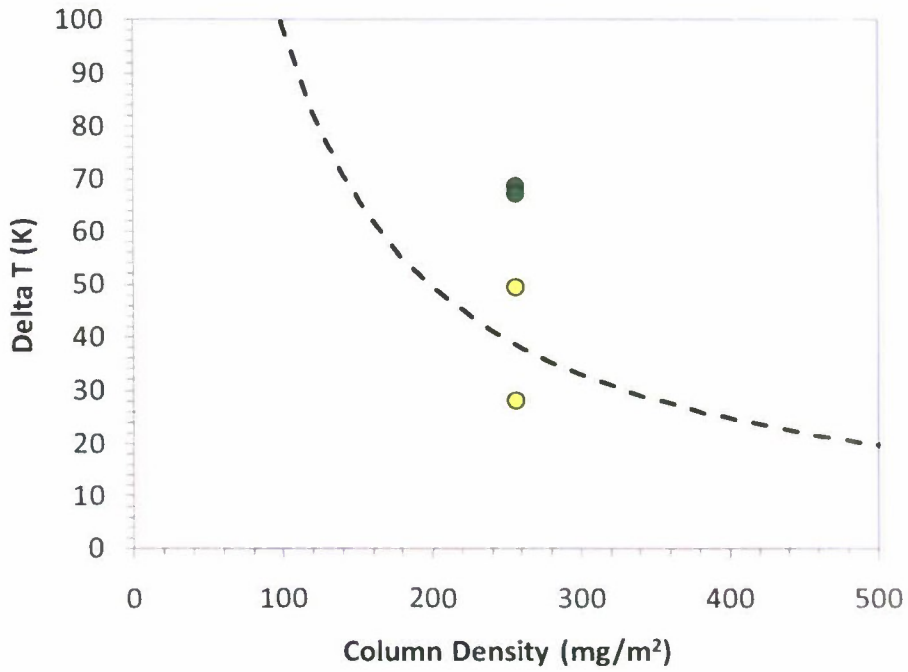

Figure 11. Graphical representation of test data (symbols) showing detection quality as a function of column density and ΔT for HD with JSLSCAD threshold limit (dashed line).

6. CONCLUSIONS

The tests described in this report provide limited data indicating that the AIRIS sensor is capable of meeting the Commercial Joint Service Lightweight Standoff Chemical Agent Detector (JSLSCAD) detection limits for GB, GD, and HD. The data provides no information on susceptibility to interferents, false alarm rates, or cross sensitivity to other agents.

Figures 12 and 13 show the absorption cross sections from the PNNL database for the nerve and blister agents listed in the JSLSCAD specifications (Table 1). This data shows that the cross sections for the strongest bands of the agents tested in the measurements described in this report are comparable in strength to the strongest bands found in Figures 12 and 13 for the nerve and blister agents that were not tested.[3-9] To the extent that detection capability is determined by the absorption strength of the target compounds, the data in this report suggests that comparable detection capability might be achieved by the sensor for those nerve and blister agents not tested in this study.

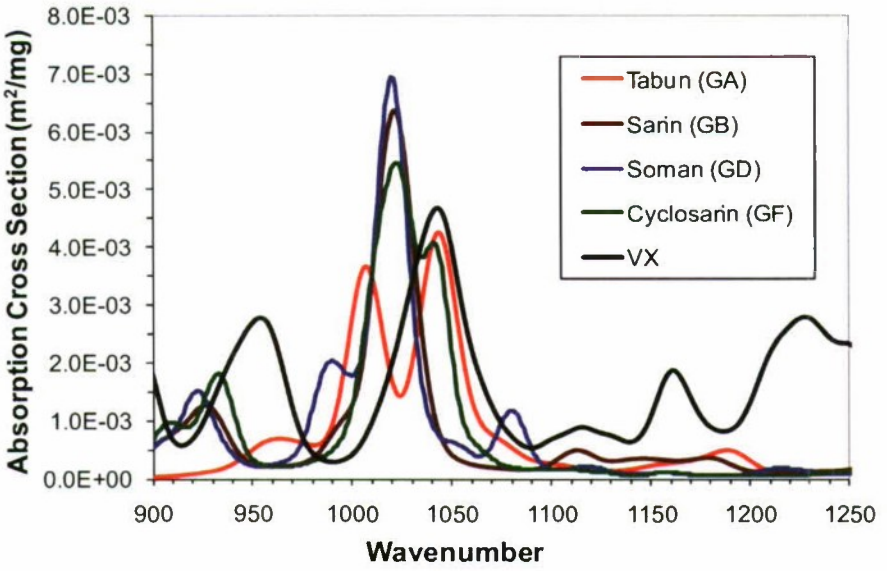

Figure 12. IR absorption spectra of nerve agents.

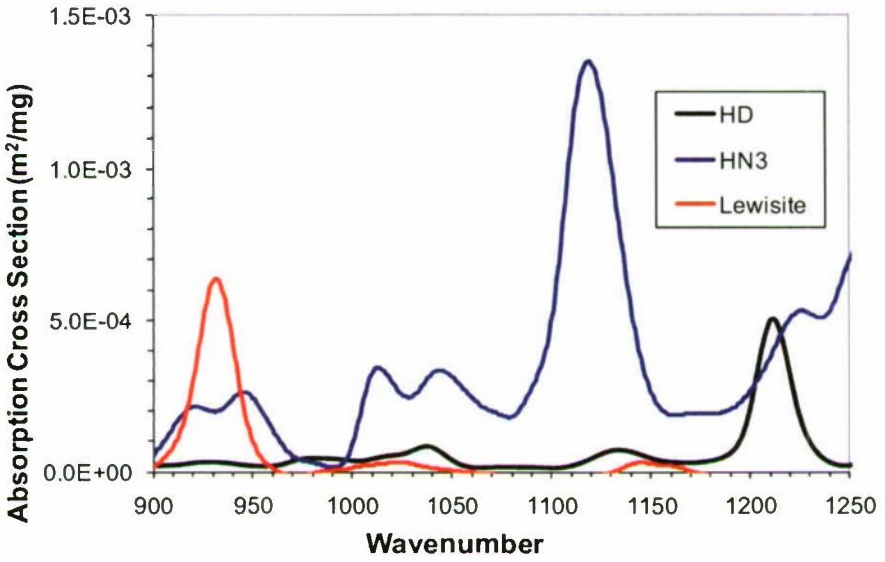

Figure 13. IR absorption spectra of blister agents.

REFERENCES

1. Tevault, D.; Keller, J.; Parsons, J. Vapor Pressure of Dimethyl Methylphosphonate, (AD-E491 779). In *Proceedings of the 1998 ERDEC Scientific Conference on Chemical and Biological Defense Research,* 17-20 November 1998; ECBC-SP-004; Berg, D.A., Compiler; U.S. Army Edgewood Chemical Biologieal Center: Aberdeen Proving Ground, MD, 1999; UNCLASSIFIED Report (AD-A375 171).

2. Williams, B.R.; Hulet, M.S.; Ben-David, A.; Miles, R.W.; Samuels, A.C.; Zhu, C.; Green, N. *Validation and Support of a Quantitative Infrared Instrument Facility and Generation of a Library of Chemical Warfare and Related Materials by Fourier Transform Infrared Spectroscopy*; ECBC-CR-076; U.S. Army Edgewood Chemieal Biological Center: Aberdeen Proving Ground, MD, 2006; UNCLASSIFIED Report (AD-A471 712).

3. Sharpe, S.W.; Johnson, T.J.; Chub, P.M.; Kleimeyer, J.; Rowland, B. Quantitative, Infrared Spectra of Vapor Phase Chemical Agents. In *Proceedings of SPIE-The International Society for Optical Engineering: Chemical and Biological Sensing IV*, 21-22 April 2003, Orlando, FL, Vol. 5085, Gardner, Patrick J., ed., pp. 19-27. SPIE , Bellingham, WA.

4. Williams, B.R.; Hulet, M.S.; Samuels, A.C. Miles, R.W. *Vapor-Phase Infrared Absorptivity Coefficient of Isopropyl Methylphosphonofluoridate*; ECBC-TR-696; U.S. Army Edgewood Chemical Biologieal Center: Aberdeen Proving Ground, MD, 2009; UNCLASSIFIED Report (AD-A501 352).

5. Williams, B.R.; Hulet, M.S.; Samuels, A.C.; Miles, R.W.; Berg, F.J.; McMahon, L.; Durst, H.D. *Vapor-Phase Infrared Absorptivity Coefficient of Bis-(2-chloroethyl) Sulfide*; ECBC-TR-638; U.S. Army Edgewood Chemieal Biologieal Center: Aberdeen Proving Ground, MD, 2008;.UNCLASSIFIED Report (AD-A487 002).

6. Williams, B.R.; Hulet, M.S.; Samuels, A.C.; Miles, R.W. *Vapor-Phase Infrared Absorptivity Coefficient of Pinacolyl Methylphosphonofluoridate*; ECBC-TR-688; U.S. Army Edgewood Chemical Biologieal Center: Aberdeen Proving Ground, MD, 2009; UNCLASSIFIED Report (AD-A500 806).

7. Samuels, A.C.; Miles, R.W.; Williams, B.R.; Hulet, M.S. *Vapor-Phase Infrared Absorptivity Coefficient of Cyclohexyl Methylphosphonofluoridate*; ECBC-TR-691; U.S. Army Edgewood Chemical Biological Center: Aberdeen Proving Ground, MD, 2006; UNCLASSIFIED Report (AD-A502 852).

8. Williams, B.R.; Hulet, M.S.; Samuels, A.C.; Miles, R.W.; Berg, F.J.; McMahon, L.; Durst, H.D. *Vapor-Phase Infrared Absorptivity Coefficient of 2-Chlorovinyl Dichloroarsine (Lewisite)*; ECBC-TR-667; U.S. Army Edgewood Chemieal Biologieal Center: Aberdeen Proving Ground, MD, 2009; UNCLASSIFIED Report (AD-A493 633).

9. Williams, B.R.; Hulet, M.S.; Samuels, A.C.; Miles, R.W. *Vapor-Phase Absorptivity Coefficient of Ethyl N,N-dimethylphosphoramidocyanidate*; ECBC-TR-732; U.S. Army Edgewood Chemical Biological Center: Aberdeen Proving Ground, MD, 2010; UNCLASSIFIED Report (AD-A513 632).